Orthodontics & Craniofacial Research

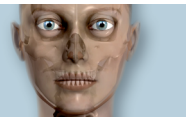

ORIGINAL ARTICLE

I. Bugaighis
C. R. Mattick
B. Tiddeman
R. Hobson

3D asymmetry of operated children with oral clefts

Authors' affiliations:
I. Bugaighis, Department of Orthodontic, Faculty of Dentistry, Benghazi University, Benghazi, Libya
C. R. Mattick, Royal Victoria Infirmary, Newcastle upon Tyne, UK
B. Tiddeman, Department of Computer Science, University of Aberystwyth, Aberystwyth, UK
R. Hobson, Private Practice, Windmill Dental Suite, Newcastle upon Tyne, UK

Correspondence to:
Dr I. Bugaighis
Department of Orthodontic
Faculty of Dentistry
Benghazi University
P.O. Box 595
Benghazi
Libya
E-mail: isbugaighis@yahoo.com

Date:
Accepted 26 May 2013

DOI: 10.1111/ocr.12026

Bugaighis I., Mattick C. R., Tiddeman B., Hobson R. 3D asymmetry of operated children with oral clefts
Orthod Craniofac Res 2014; **27**: 27–37. © 2013 John Wiley & Sons A/S. Published by John Wiley & Sons Ltd

Structured Abstract

Objectives – To explore three-dimensional (3D) facial asymmetry differences in operated children with oral clefts and to compare the results with a control group.

Setting and Sample Population – The sample comprised one hundred and three 8- to 12-year-old children: 40 with unilateral cleft lip and palate (UCLP); 23 with unilateral cleft lip and alveolus (UCLA); 19 with bilateral cleft lip and palate (BCLP); 21 with cleft palate (CP) and 80 sex- and age-matched controls living in the North East of England.

Materials and Methods – 3D stereophotogrammetric facial scans were recorded for each participant at rest. Thirty-nine landmarks were recorded for each scan. The *x*, *y* and *z* coordinates for each landmark were extracted. Kruskal–Wallis and Mann–Whitney tests were conducted to identify 3D landmark asymmetry differences between the groups.

Results – Statistically significant differences were observed between all the groups. The UCLP and UCLA patients displayed the greatest asymmetry, followed by the BCLP group. The CP group was the least asymmetric among the cleft groups. Asymmetry was present to a lesser extent in the control group.

Conclusions – Shape analysis indicates the possible differences in the aetiology and growth pattern of the CP group compared to UCLA or UCLP and BCLP groups.

Key words: 3D imaging; asymmetry; cleft lip and palate; shape analysis

Introduction

Cleft lip and palate is the most commonly occurring craniofacial anomaly (1), with approximately one in 700 new born babies affected in the United Kingdom (UK) (2). Subjects with oral clefts have different facial shapes compared to their unaffected

peers. These differences vary according to both the type of cleft and also the cleft repair surgical technique used (3). There are profound clinical and psychological consequences of oral clefts for breathing, swallowing, mastication, osculation and speech (4), with facial asymmetry being one of the common features of oral clefts involving the lip (5–7).

The application of a centralized multidisciplinary protocol in the management of oral clefts in the UK has increased the demand for the assessment of treatment outcomes. The development of accurate 3D surface imaging systems and powerful statistical tools for shape analysis is of potential significance in the evaluation of these outcomes.

Mild asymmetry is a common biological characteristic and can be found even in aesthetically pleasing faces (5, 8, 9). Conversely, equal paired linear measurements can be found even between asymmetrical paired landmarks (6, 10). Studies assessing facial asymmetry have used two-dimensional paired radiographic measurements (11), photographic surfaces (12) and paired anthropometric linear measurements (8, 13–15). Indirect three-dimensional (3D) Automated infrared photogrammetry (16) and construction of midfacial plane of symmetry have also been used (7). Garrahy (6) assessed the effect of oral clefts on facial asymmetry using 3D Procrustes analysis. She presented the results in unit size instead of millimetres (mm) to which the facial landmark configurations were scaled. Recently, Bugaighis et al. (17) reported a new method of quantifying facial asymmetry in male and female subjects (8–12 years old) by using the best fit between an original 3D image scan and a reflected 3D image with generalized Procrustes analysis (GPA). The distance was quantified in millimetre between the original and reflected landmarks.

The aim of this study was to examine the extent of 3D facial asymmetry of children with unilateral cleft lip and palate (UCLP), bilateral cleft lip and palate (BCLP), unilateral cleft lip and alveolus (UCLA) and cleft palate (CP) and a matched control group using 3D data acquisition media and statistical shape analysis. The null hypothesis tested was that there are no significant differences in 3D landmark asymmetry between subjects with UCLP, UCLA, BCLP, CP and a matched control group.

Materials and methods

Approval was secured from the Research Ethics Committee (06/Q0902/36) and written and verbal informed consent was obtained from parents/guardians and children. The investigation was conducted on 103 children aged 8–12 with nonsyndromic operated oral clefts and 80 sex- and age-matched controls. The cleft group comprised 40 subjects with UCLP (mean age 10.1 years, SD = 1.5); 23 with UCLA (mean age 10 years, SD = 1.2); 19 with BCLP (mean age 10 years, SD = 1.3); and 21 with CP (mean age 10 years, SD = 1.5). All subjects examined were Caucasian in origin and living in the North East of England. The enrolled subjects with oral clefts were drawn from the cleft multidisplinary clinics coordinated by the Royal Victoria Infirmary in the North East of England. The clefts were repaired prior to the implementation of the Clinical Standards Advisory Group (CSAG) (18) recommendations where five different surgeons using different protocols were involved in cleft repair during the first year of the children's lives. The exact surgical procedures followed could not be determined due to poor documentation at that time. Clefts in children with UCLP and BCLP were complete and alveolar bone grafting procedures had not been performed. All children in the control group (mean age 10.5 years, SD = 1.3) were drawn from the Child Dental Health Department at Newcastle Dental Hospital. The control group was recruited from the Child Dental Health Department if individuals presented with harmonious balanced faces with a Class I dental occlusion, competent lips and no craniofacial abnormalities, including hypodontia. Any child in the control group who had undergone orthodontic treatment was excluded. The study was designed to increase the number of subjects in the control group to increase the power of the analysis between

controls and the cleft groups (19). This sample size has a 90% power to detect an effect size (standardized difference) of 0.85 assuming a Type I error rate of 5%. In the present study, the smaller number of children in the cleft groups did not allow an assessment of both sexes separately to be performed.

Image acquisition and processing

3D photorealistic facial scans were captured for each subject by a non-invasive 3D stereophotogrammetry system (3dMD, Atlanta, GA, USA) comprising two modular units with two pods containing six cameras, two high-resolution stereopairs of digital geometry cameras, a stereopair of high-resolution texture cameras (2 megapixels) and one stereopair of infrared projectors. In addition, there is a stereopair of texture flashes to illuminate the subject.

Subjects were seated 95 cm in front of the unit with the Frankfort plane raised anteriorly by ten degrees to the horizontal to ensure a clear picture of the nose. The subjects were instructed to be at rest with lips lightly opposed (if possible without straining), at rest and with eyes open without stretching the forehead. All cameras and flashes were synchronized to capture the entire surface of the face from ear to ear, simultaneously generating one continuous point cloud. Image capture time was two milliseconds, which minimized changes in position or facial expression. Four geometrical and two texture images were recorded for each child. Subsequently, the captured images were processed in a connected computer to generate triangulation of data geometry, constructed from the captured point cloud. In each case, the captured image comprised approximately 40 000 vertices, allowing construction of a polygonal mesh model of the recorded face with a resolution of two megapixels.

Landmark identification

Scans with right unilateral clefts were reflected using MorphAnalyser so as to always keep the cleft side on the left for uniformity of analysis. Thirty-nine anthropometric homologous landmarks were recorded for each scan to evaluate facial (Fig. 1) and especially nasolabial form (Figs 2 and 3). The landmarks used were selected mainly based on work by Farkas (20) (Table 1) and were recorded using MorphAnalyser software (V 2.07; user.aber.ac.uk/bpt) (21). MorphAnalyser is an original 3D software package developed by Tiddeman et al. (21) that allows import of 3D facial scans, digitization of landmarks and extraction of the *x*, *y* and *z* coordinates of each landmark. The software

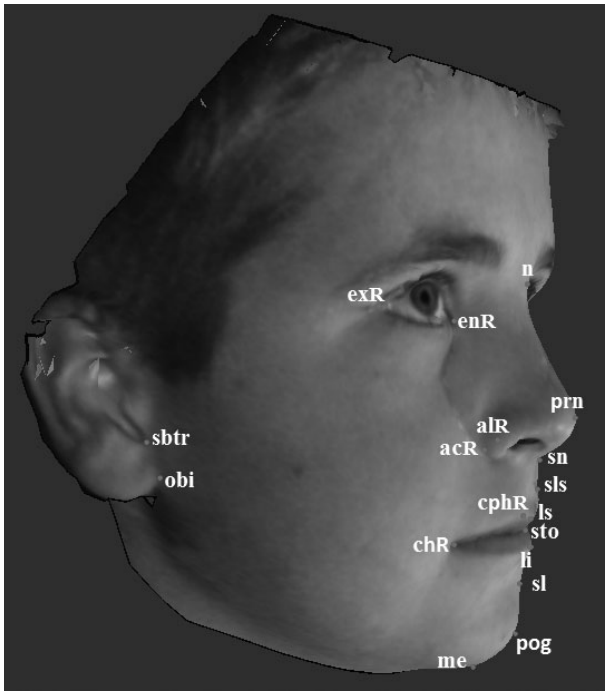

Fig. 1. 3D facial anthropometric landmarks.

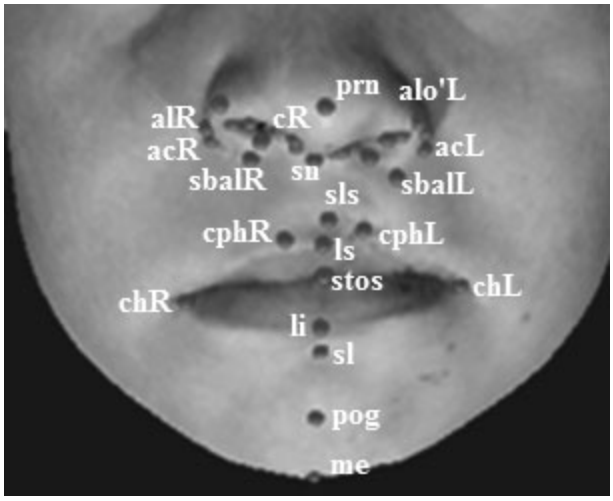

Fig. 2. 3D nasolabial landmarks.

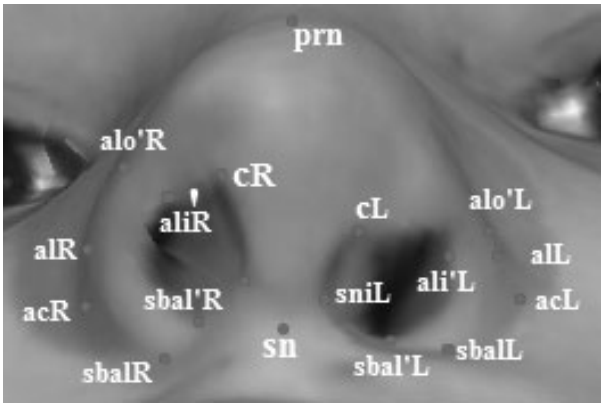

Fig. 3. 3D nasal landmarks.

facilitates the matching of corresponding surfaces between specified landmarks, allowing the construction of averages using principle component analysis (PCA) of surface shape and probabilistic analysis of local surface shape. It also provides a number of operations on landmark points such as measurement of lengths and angles and assessment of landmark asymmetry. *In vitro* and *in vivo* error assessment studies were conducted. Error from image acquisition, MorphAnalyser software and operator error was, on average, 0.5 mm (22). This value was comparable with that of other 3D morphometric validation studies (6, 23).

3D asymmetry

The 3D asymmetry of facial landmarks was assessed by reflecting each facial scan and comparing the original and reflected versions using GPA for translating, rotating and scaling them to best fit while retaining their shape. The distance between each landmark and the matching reflected landmark was calculated in millimetre and the asymmetry was evaluated for each landmark. To undertake this procedure, the corresponding left–right landmarks were specified interactively on each image and saved. The midsagittal landmarks were considered to be their own mirror image. Once the symmetric point pairs had been specified, different sets of landmark points could be identified and measurement of asymmetry calculated in mm.

Statistical analysis

The Statistical Package of the Social Sciences Software (SPSS Inc., Chicago, IL, USA) version 15.0 was used. The symmetry of 11 midsagittal and 14 paired landmarks were assessed in each subject.

For all linear variables, the Shapiro–Wilk test revealed that the data were significantly different from a normal distribution. The Levene test established the variances to be nonhomogeneous. Nonparametric tests were applied to compare 3D landmark asymmetry between controls and all cleft groups. Multiple comparisons of the levels of 3D landmark asymmetry in all groups were undertaken using Kruskal–Wallis and Mann–Whitney tests. In the Mann–Whitney test, the Bonferroni correction was applied to control the Type I error rate. This was undertaken by dividing the critical p value for significance by the number of groups included in the study.

Results

3D landmark asymmetry

Tables 2 and 3 display the 3D landmark asymmetry (in mm) and the p values for the control group and the cleft groups.

Controls compared to UCLP

The facial surface determined for UCLP was the most asymmetric of the examined groups. Statistically significant differences in the symmetry of all 3D landmarks were found between the control and UCLP groups ($p \leq 0.001$) with the most apparent differences being in the nasolabial region. Interestingly, the aural region landmark asymmetry, with a mean value of 2.47 mm, was similar to most of the nasolabial region in the UCLP group, but the significantly greater distance between the paired landmarks made this asymmetry less noticeable. Also, the control group had greater asymmetry in the aural region relative to the other control facial landmarks, with a mean asymmetric value of 1.52 mm.

Table 1. **Definition of the facial soft tissue landmarks used in the study**

Landmarks (R = Right, L = Left)	Definitions
Upper face landmarks	
Exocanthion *(exR, exL)*	Located at the outer commissure of the eye fissure
Endocanthion *(enR, enL)*	Located at the inner commissure of the eye fissure
Nasion *(n)*	Point in the midline of the nasal root identical to hard tissue nasion
Nasolabial landmarks	
Alare curvature *(acR, acL)*	Most lateral point in the curved base line of each ala
Alare *(alR, alL)*	Most lateral point on each alar contour where nostril commence to be curved laterally
Columellar high point *(cR, cL)*	Highest point on columella crest
Inner alare *(ali'R, ali'L)*	Inner marking level at the midportion of the alae where the thickness of each ala is measured
Outer alare *(alo'R, alo'L)*	Outer marking level at the midportion of the alae where the thickness of each ala is measured
Pronasale *(prn)*	Most protruded point of the apex of the nose
Subalare *(sbalR, sbalL)*	Point at the lower limit of each alar base where it joins the skin of the upper lip
Subalare' *(sbali'R, sbali'L)*	Point at the inner lower limit of each alar base
Subnasale *(sn)*	Midpoint of maximum concavity where upper lip skin meets columella base
Subnasale inner *(sniR, sniL)*	Midpoint of columella on each side at the bottom line where the thickness of the columella is measured
Cheilion (chR-chL)	Point located at each labial commissure
Christa philtri *(cphR, cphL)*	Point on each elevated margin of upper lip at the junction of vermillion line of upper lip and white roll line
Laberale superiorus *(ls)*	Midpoint of upper vermillion line
Laberale inferiorus *(li)*	Midpoint of the lower vermillion line
Superior labial sulcus *(sls)*	Deepest midline point between the mouth and the nose
Stomion Superiorus *(stos)*	Most inferior midpoint of the vermillion border of the upper lip
Stomion inferiorus *(stoi)*	Most superior midpoint of the vermillion border of the lower lip
Lower face landmarks	
Sublabialis *(sl)*	Determines lower border of the lower lip and the upper border of the chin
Pogonion *(pog)*	The most anterior midpoint of the chin
Menton *(me)*	The lowest median point on the lower border of the mandible
Aural landmarks	
Subtragion *(strR, strL)*	Most inferior point on the anterior inferior margin of the helix attachment of the face
Otobasion inferiorus *(obiR, obiL)*	Most inferior point on the ear lobe at the attachment to the cheek

Differences were found in the upper facial region of the UCLP face, where the outer and inner contours of the eye and the midline of the nasal root were significantly asymmetric, with a mean of 1.60 mm compared to the control group (mean asymmetry of 0.93 mm; $p < 0.001$). The exocanthion landmark was the most asymmetric in the upper facial region of the control group (1.34 mm).

In the nasal region, the displaced dome of the nose showed the greatest asymmetric difference between the UCLP (*prn* = 4.11 mm) and control groups (0.44 mm). Furthermore, the whole nasal surface showed significant asymmetry for the ten recorded nasal landmarks, with a mean asymmetry of 3.00 mm compared to the control group, which showed mean asymmetry of 0.69 mm ($p < 0.001$).

The upper lip and philtrum were significantly asymmetric in the UCLP group, as demonstrated by six recorded landmarks, which displayed mean asymmetry of 2.36 mm compared to the

Table 2. **Medians and interquartiles (mm) of 3D landmarks asymmetry and p values of the control and cleft groups using Kruskal–Wallis analysis at $p < 0.05$**

				Cleft groups												
	Control			UCLP			UCLA			BCLP			CP			
Landmarks	25th	Median	75th	25th	Median	75th	25th	Median	75th	25th	Median	75th	25th	Median	75th	*p*
Exocanthion *(ex)*	0.86	1.34	1.74	1.47	1.99	2.68	1.19	1.95	2.35	1.04	1.42	2.73	0.98	1.53	2.58	<0.001
Endocanthion *(en)*	0.75	1.009	1.26	1.28	1.64	2.35	1.00	1.35	1.97	0.77	1.40	2.20	0.77	1.08	1.78	<0.001
Nasion *(n)*	0.26	0.46	0.88	0.67	1.16	1.64	0.67	1.17	1.76	0.40	0.72	1.01	0.21	0.66	1.61	<0.001
Sublabialis *(sl)*	0.20	0.38	0.70	0.59	0.74	1.42	0.26	0.88	1.17	0.41	1.02	1.36	0.42	0.54	0.87	<0.001
Pogonion *(pog)*	0.13	0.30	0.62	0.37	0.82	1.10	0.30	0.66	1.67	0.52	0.88	1.19	0.24	0.62	1.02	<0.001
Menton *(me)*	0.31	0.47	0.71	0.43	0.83	1.51	0.47	0.82	1.61	0.17	0.84	1.48	0.50	0.65	1.48	<0.001
Subtragion *(sbtr)*	1.01	1.41	2.05	1.73	2.50	3.40	1.50	1.92	3.01	1.33	1.68	3.18	1.27	1.74	2.44	<0.001
Otobasion inferiorus *(obi)*	1.00	1.62	2.12	1.58	2.43	2.97	0.81	1.85	3.15	1.35	2.05	3.20	1.08	1.75	2.18	0.008
Pronasale *(prn)*	0.21	0.44	0.80	2.72	4.11	5.33	1.99	3. 06	4.48	0.67	1.64	3.02	0.18	0.52	0.88	<0.001
Subnasale *(sn)*	0.16	0.43	0.74	0.87	2.31	3.37	1.07	1.58	3.65	0.48	0.83	2.15	0.23	0.44	0.76	<0.001
Alare *(al)*	0.67	0.86	1.05	2.05	3.06	3.92	1.53	2.09	2.59	1.01	2.03	2.50	0.58	0.84	1.07	<0.001
Alare curvature *(ac)*	0.63	0.80	1.09	1.68	2.23	3.35	1.42	1.63	2.18	1.34	2.00	2.42	0.66	1.07	1.41	<0.001
Subalare *(sbal)*	0.57	0.70	0.85	2.08	2.95	3.44	1.38	1.75	3.24	1.38	1.95	2.40	0.72	0.98	1.38	<0.001
Subalare'*(sbal')*	0.52	0.72	0.90	2.05	2.77	3.54	1.64	2.20	2.88	1.55	2.14	2.59	0.54	0.89	1.36	<0.001
Columella *(c)*	0.49	0.66	0.92	2.36	3.28	4.10	1.94	2.53	3.91	1.19	2.22	3.95	0.45	0.71	1.22	<0.001
Alare outer *(alo')*	0.68	0.83	1.04	2.44	3.32	4.32	2.29	2.94	3.20	1.65	2.54	3.43	0.77	0.98	1.36	<0.001
Alare inner *(ali')*	0.58	0.75	1.01	2.19	3.17	3.89	2.02	2.58	3.25	1.37	1.80	3.00	0.63	0.89	1.28	<0.001
Subnasale' *(sn')*	0.42	0.67	0.87	1.60	2.79	3.63	1.59	2.40	3.27	1.06	1.27	2.00	0.49	0.74	1.05	<0.001
Christa philtri *(cph)*	0.43	0.59	0.82	1.91	2.91	3.41	1.00	2.08	4.79	0.96	1.44	1.78	0.71	1.07	1.92	<0.001
Cheilion *(ch)*	0.93	1.17	1.60	2.03	2.54	3.54	1.41	2.03	3.19	1.12	1.56	2.46	1.18	1.61	2.20	<0.001
Superior nasale sulcus *(sls)*	0.24	0.41	0.72	0.55	1.54	3.11	0.70	1.74	2.66	0.25	0.72	1.29	0.42	0.72	0.99	<0.001
Laberale superiorus *(ls)*	0.21	0.39	0.75	1.25	1.68	3.20	1.33	1.97	4.31	0.16	1.02	1.52	0.50	0.73	1.04	<0.001
Stomion superiurus *(stos)*	0.14	0.30	0.58	1.09	1.56	2.55	0.82	1.98	3.81	0.44	0.99	1.85	0.38	0.73	0.95	<0.001
Stomion inferiorrus *(stoi)*	0.11	0.28	0.58	0.76	1.44	2.19	0.44	1.05	1.91	0.38	0.82	2.04	0.31	0.68	0.92	<0.001
Laberale inferiorus *(li)*	0.16	0.35	0.58	0.73	1.08	1.57	0.34	0.88	1.91	0.44	0.80	2.03	0.42	0.62	0.84	<0.001

Table 3. **Comparison of 3D landmark asymmetry for the controls and the individual cleft groups ($p < 0.01$) using Mann–Whitney tests**

Landmarks	Pairwise comparison between the children's groups									
Exocanthion *(ex)*	Control	V	UCLP	<0.001	UCLA	0.004				
Endocanthion *(en)*	Control	V	UCLP	<0.001	UCLA	0.001	BCLP	0.006		
Nasion *(n)*	Control	V	UCLP, UCLA	<0.001						
Sublabialis *(sl)*	Control	V	UCLP, BCLP	<0.001						
Pogonion *(pog)*	Control	V	UCLP, BCLP	<0.001	UCLA	0.002				
Menton *(me)*	Control	V	UCLP	0.001	UCLA	0.005	BCLP	0.006	CP	0.007
Subtragion *(sbtr)*	Control	V	UCLP	<0.001						
Otobasion inferiorus *(obi)*	Control	V	UCLP	0.001						
Pronasale *(prn)*	Control	V	UCLP, UCLA, BCLP	<0.001						
Subnasale *(sn)*	Control	V	UCLP, UCLA	<0.001	BCLP	0.003				
Alare *(al)*	Control	V	UCLP,UCLA, BCLP	<0.001						
Alare curvature *(ac)*	Control	V	UCLP,UCLA, BCLP	<0.001						
Subalare *(sbal)*	Control	V	UCLP, UCLA, BCLP	<0.001	CP	0.003				
Subalare' *(sbal')*	Control	V	UCLP, UCLA, BCLP	<0.001						
Columella *(c)*	Control	V	UCLP, UCLA, BCLP	<0.001						
Alare outer *(alo')*	Control	V	UCLP, UCLA, BCLP	<0.001						
Alare inner *(ali')*	Control	V	UCLP, UCLA, BCLP	<0.001						
Subnasale' *(sn')*	Control	V	UCLP, UCLA, BCLP	<0.001						
Christa philtri *(cph)*	Control	V	UCLP, UCLA, BCLP, CP	<0.001						
Cheilion *(ch)*	Control	V	UCLP, UCLA	<0.001	BCLP	0.006	CP	0.004		
Laberale superiorus *(ls)*	Control	V	UCLP, UCLA	<0.001	CP	0.004				
Superior labial sulcus *(sls)*	Control	V	UCLP, UCLA	<0.001						
Stomion superiorus *(stos)*	Control	V	UCLP, BCLP, UCLA	<0.001	CP	0.001				
Stomion inferiorus *(stoi)*	Control	V	UCLP, UCLA, BCLP	<0.001	CP	0.005				
Labialis inferiorus *(li)*	Control	V	UCLP, UCLA, BCLP	<0.001	CP	0.001				

control baseline (mean asymmetry of 0.54 mm). The oral asymmetry in the UCLP group was assessed by six landmarks; these showed a mean asymmetry of 1.87 mm compared to landmarks in the control group (mean asymmetry of 0.51 mm). In the lower face (excluding the lower lip), the difference between mean landmark asymmetry in the UCLP group (0.80 mm) and that of the control group (0.38 mm) was also statistically significant ($p \leq 0.001$).

Controls compared to UCLA

Greater facial asymmetry was observed in the UCLA group, both in the nasolabial region ($p < 0.001$) and the chin area ($p \leq 0.005$). Unlike the UCLP group, the UCLA aural region asymmetry (mean = 1.89 mm) was similar to the aural surface in the control group with a mean value of 1.52 mm ($p \geq 0.026$). The upper UCLA face was significantly asymmetric (mean asymmetry of 1.49 mm) compared to the control group (mean asymmetry of 0.93 mm; $p \leq 0.004$).

The most asymmetric facial surface was found on the displaced dome of the nose (*prn* = 3.06 mm, compared to the control group value of 0.44 mm; $p < 0.001$). The entire nasal surface was significantly more asymmetric in this group. This was seen in the asymmetry of the ten recorded landmarks on the nasal surface with mean asymmetry of 2.28 mm compared to the control group, in which mean asymmetry was 0.69 mm ($p < 0.001$).

The UCLA philtrum and upper lip were also more asymmetric than controls: mean asymmetry of 1.89 mm was observed in the experimental

sample, compared to the control baseline mean asymmetry of 0.54 mm ($p \leq 0.002$). Oral asymmetry in the UCLA group was assessed by six recorded landmarks with mean asymmetry of 1.67 mm compared to mean asymmetry of 0.51 mm in the control group ($p < 0.001$). The sublabialis region was similar in both groups ($p = 0.136$), but the UCLA chin region, with mean asymmetry of 0.74 mm, was more asymmetric than in control group (mean asymmetry of 0.385 mm; $p \leq 0.005$).

Controls compared to BCLP

The BCLP face showed a lesser degree of asymmetry compared to the unilateral cleft groups, with nineteen significantly asymmetric landmarks out of 25. The only asymmetric difference in the BCLP upper face was in the inner ocular contour surface (*en* = 1.40 mm; control group: *en* = 0.99 mm; $p = 0.006$). However, all ten recorded nasal landmarks were asymmetric in the BCLP face compared to the control group ($p \leq 0.003$). The nasal rim and the upper part of the columella surface were more asymmetric (mean landmark asymmetry: 2.10 mm) than the assumed nasal midline (mean asymmetry: 1.24 mm) and the control group nasal rim and upper columella (mean asymmetry: 0.76 mm). Moreover, the BCLP *sn'* landmark (*sn'* = 1.27 mm) was more asymmetric than in the control group at 0.67 mm ($p < 0.001$).

The BCLP upper lip and philtrum surface asymmetry (mean = 1.35 mm) was greater than that observed for the corresponding surfaces in the control group (mean = 0.54 mm) at $p \leq 0.003$, except for the superior labial sulcus (*sls*) and labialis superiorus (*ls*) landmarks, where asymmetry was similar in both groups. For the six recorded oral landmarks, asymmetry of BCLP faces (mean = 1.11 mm) was greater than the corresponding landmarks in the control group (mean = 0.51 mm), all of which differences were significant ($p \leq 0.006$) except for the *ls* landmark ($p = 0.025$). Greater asymmetry was also found for the BCLP lower facial landmarks (mean = 0.91 mm; control group: mean = 0.38 mm; $p \leq 0.006$). However, in the case of aural landmarks, asymmetry was similar in both the BCLP and control groups ($p \leq 0.033$).

Controls compared to CP

Eight of 25 landmarks were asymmetric in CP subjects compared to the control group ($p \leq 0.007$), all of which were in the nasolabial area, except for the menton landmark (*me* = 0.65 mm; control group: 0.47 mm; $p = 0.007$). Similar asymmetry was found in the upper face and aural landmarks in both groups ($p \geq 0.110$). The surface of the insertion of the alar wing to the upper lip (*sbal* = 0.98 mm) was the only asymmetric nasal landmark in the CP face (control: *sbal* = 0.70 mm; $p = 0.003$). The mouth was the most asymmetric surface in the CP face with a mean landmark asymmetry of 0.92 mm (control group mean landmark asymmetry: 0.47 mm; $p \leq 0.005$).

Discussion

This is the first indirect morphometric study applying advanced statistical tools to investigate 3D facial asymmetry occurring within and between the four main cleft groups. It goes further than previous UK-based studies by including more groups with oral clefts and control subjects, by controlling data acquisition, and by using advanced non-invasive 3D technology while focusing on one centre. Thus, for example, Shaw et al. (24) examined 151 British children with UCLP of a similar age to those in the present research (8–11 years) in a retrospective cross-sectional noncontrolled cohort study to compare cleft repair surgical outcome between six British centres. The number of subjects ranged between 23 and 26 from each centre. The authors compared craniofacial form, dental arch relationships and nasolabial appearance, but their research employed 2D acquisition tools, losing the third dimension. In the present study, 3D facial asymmetry was assessed by quantifying (in mm) the distance between each landmark and the corresponding reflected point

without relying on a symmetrical facial plane. This allowed the assessment of the contribution of each facial region to the overall facial asymmetry. However, the results did not provide information about whether asymmetry is greater in the *x, y* or *z* direction and it would be of interest to investigate this further.

Unfortunately, the association between age and symmetry could not be investigated in the present study as this would have rendered the cleft groups yet smaller. Separate analysis for males and females in the cleft groups could not be undertaken for similar reasons. It will be interesting to investigate these factors in a larger study with increased sample size.

Facial asymmetry was more pronounced in the cleft groups, although the control group faces were not perfectly symmetric, with the control aural region being most asymmetric. The mid-sagittal landmarks in the control group were less asymmetric and their asymmetric values were within the range of the landmark reproducibility error. However, when the images were superimposed, the landmarks did not correspond with their reflections. A detailed description of male and female landmark asymmetry had been published in previous study (17).

The UCLA group showed significant landmark asymmetry, although less than the UCLP group. The asymmetry in both cleft types was mainly due to the unilateral nature of the deformity and its repair involving the lip/alveolus; therefore, a greater effect on facial appearance/symmetry is expected compared to the BCLP and CP groups. Hood (23) reported similar results, with the UCLP facial soft tissue more asymmetric than that in the UCL group and both cleft types more asymmetric than controls. Both the Hood (23) and present study subjects had been operated on following heterogeneous surgical protocols. On the other hand, Garrahy (6) found similar asymmetry scores at 3 years of age in both her UCLP and UCL groups, who had all undergone operations using a single surgical technique, were similar, although still greater than in the controls. She found that the asymmetry in her cleft groups was mainly in the upper lip and the nasal base, while the upper face and nasal prominence landmark asymmetry was similar to her control group. Stauber et al. (25) found that the asymmetry in 10-year-old German children with UCLP, who were operated on following a single surgical technique, was confined to the nasal landmarks; the oral and endocanthion landmarks were symmetrical. The heterogeneous surgical protocols followed in the treatment of the present and Hood (23) samples might therefore have contributed to the reported differences in results.

The extension of the cleft to involve the palate in the UCLP group accentuated facial soft tissue asymmetry. This was confirmed by the high asymmetry values of all the recorded landmarks in the UCLP group compared to the other examined groups. The significant difference in the UCLP endocanthion landmark asymmetry might be caused by the extension of the unilateral cleft effect to a higher level involving the orbits leading to displacement of the soft tissue around the inner ocular region on the affected side. However, this assumption will need to be reassessed in further studies where the significantly asymmetric nasolabial landmarks are excluded to avoid their influence on the upper face.

BCLP is a more symmetrical defect than a single-sided cleft and accordingly this group had less asymmetric faces than those in the unilateral cleft groups (ULP and UCLA), although significantly more asymmetric than the CP group faces. In the nasolabial region of the BCLP group, paired landmarks were more asymmetric than the midline landmarks, possibly because the cleft had displaced the adjacent muscle fibres and the overlying soft tissue to a greater extent than in the more distal midline area. Alternatively, the surgical repair could have succeeded in enhancing the soft tissue symmetry in the area closer to the midline more than in the region nearer to the deformity.

A midline cleft of the soft and hard palate (CP) is not a highly asymmetric defect, nor does it directly affect the anterior maxilla or overlying soft tissue as do both unilateral and bilateral cleft lip/alveolus; therefore, CP is expected it to have the least effect on facial appearance/symmetry compared to the other cleft groups. Accordingly,

the landmark asymmetry in the present CP group was the most similar to controls, compared to the other cleft groups. Farkas and Lindsay (14) found that 16- to 20-year-old subjects with CP had a high incidence of nasal deformity, which was interpreted as the possible presence of 'microform' cleft lip. In this study, the palate defect had more consequences for the asymmetry of the oral soft tissue than the nasal structures, and this would seem to be more consistent with the presence of a microform cleft lip. However, the differences in age and sample ethnicity between the Farkas and Lindsay (14) and present studies might have contributed to these discrepancies. Unfortunately, the published 3D morphometric studies on BCLP and CP groups are sparse (14, 26), which limits further comparisons.

The examined subjects were operated by five plastic surgeons using heterogeneous techniques prior to the implementation of the CSAG recommendation (18), and because of the retirement of some surgeons, as well as poor documentation at that time (27), it was not possible to ascertain the lip and palate repair protocols used. Although the finding that combined lip and palate cleft defects have greater consequences for facial symmetry than cleft palate alone is expected, as cleft palate is a deformity in the midline while lip/alveolus clefts are not, the present assessment method shows promise for discriminating between the influence of different cleft repair techniques on craniofacial growth and development. It will be of interest in this regard to compare the reported asymmetric outcomes with the findings obtained from other centres in the UK. Current improvement in cleft management in the UK will facilitate large-scale studies that might offer better understanding of surgical outcomes.

Conclusions

In this study, the null hypothesis – that there are no differences in 3D landmark asymmetry between subjects with UCLP, UCLA, BCLP, CP and controls – could be rejected. It is concluded that a midline cleft of the soft and hard palate (CP) that does not extend to involve the lip/alveolus has the least effect on facial appearance/symmetry compared to the other cleft types. Similarly, a bilateral asymmetrical cleft involving the lip/alveolus is a more symmetrical defect than a single-sided clef, which gives rise to the most asymmetric faces, in accordance with expectations.

Furthermore, the present research confirmed that statistical shape analysis is a sensitive tool for the exploration of differences in 3D facial asymmetry between subjects with UCLP, UCLA, BCLP, CP and matched control groups.

Clinical relevance

Facial asymmetry is one of the most stigmatizing consequences of oral clefts. The assessment of the extent and the exact location of the asymmetry is usually challenging to the surgeon and orthodontist. The availability of a 3D non-invasive, transportable imaging system that can be accommodated in clinics and the relative feasibility of use of incorporated software opens new perspectives in using the present analysis routinely to quantify 3D asymmetry in conventional metric value. This would provide the surgeon with an accurate reference for reconstruction of deformed regions, so they would be similar to the unaffected reflected parts of the face.

References

1. Sampson PD, Streissguth AP, Bookstein FL, Little RE, Clarren SK, Dehane P et al. Incidence of fetal alcohol syndrome and prevalence of alcohol-related neurodevelopmental disorder. *Teratology* 1997;56:317–26.
2. Bellis T, Wohlgemuth B. The incidence of cleft lip and palate deformities in the south-east of Scotland. *Br J Orthod* 1999;26:121–5.
3. Bardach J. Anthropometry in cleft lip and palate research. In: Farkas LG, editors. *Anthropometry of the Head and Face*. New York: Raven Press; 1994. pp. 113–24.
4. Sperber G. Basic embryology of cleft lip and palate: from origin to treatment. In: Wyszynski D, editor. *Cleft Lip and Palate: From Origin to Treatment*. New York: Oxford University Press; 2002. pp. 5–24.
5. Bugaighis I, O'Higgins P, Tiddeman B, Mattick C, Ben Ali O, Hobson R. Three-dimensional geometric morphometrics applied to the study of children with cleft lip

and/or palate from the North East of England. *Eur J Orthod* 2010;32:514–21.
6. Garrahy A. 3D assessment of dentofacial deformity in children with oral clefts. Thesis, University of Glasgow; 2002. http://theses.gla.ac.uk/1475/
7. Ras F, Habets LL, van Ginkel FC, Prahl-Andersen B. Three-dimensional evaluation of facial asymmetry in cleft lip and palate. *Cleft Palate Craniofac J* 1994;31:116–21.
8. Farkas LG, Cheung G. Facial asymmetry in healthy North American Caucasians. An anthropometrical study. *Angle Orthod* 1981;51: 70–7.
9. Ferrario VF, Sforza C, Poggio CE, Tartaglia G. Distance from asymmetry: a three-dimensional evaluation of facial asymmetry. *J Oral Maxillofac Surg* 1994;52:1126–32.
10. Shaner DJ, Peterson AE, Beattie OB, Bamforth JS. Assessment of soft tissue facial asymmetry in medically normal and syndromic-affected individuals by analysis of landmarks and measurements. *Am J Med Genet* 2000;93:143–54.
11. Ishiguro K, Krogman WM, Mazaheri M, Harding RL. A longitudinal study of morphological craniofacial patterns via P-A x-ray headfilms in cleft patients from birth to six years of age. *Cleft palate J* 1976;13:104–26.
12. Coghlan BA, Mathews B, Pigott RW. A computer-based method of measuring facial asymmetry. Results from an assessment of the repair of cleft lip deformities. *Br J Plast Surg* 1987;40:371–6.
13. Farkas LG, Lindsay WK. Morphology of the adult face following repair of bilateral cleft lip and palate in childhood. *Plast Reconstr Surg* 1971;47:25–32.
14. Farkas LG, Lindsay WK. Morphology of adult face after repair of isolated cleft palate in childhood. *Cleft palate J* 1972;9:132–42.
15. Farkas LG, Lindsay WK. Morphology of adult face following repair of unilateral cleft lip and palate in childhood. *Plast Reconstr Surg* 1973;52:652–5.
16. Ferrario VF, Sforza C, Ciusa V, Dellavia C, Tartaglia GM. The effect of sex and age on facial asymmetry in healthy subjects: a cross-sectional study from adolescence to midadulthood. *J Oral Maxillofac Surg* 2001;59:382–8.
17. Bugaighis I, Mattick C, Tiddeman B, Hobson R. Three dimensional gender differences in facial form of children in the North East of England. *Eur J Orthod* 2013;35:295–304.
18. Clinical Standard Advisory Group (CSAG). *Cleft lip and/or Palate*. London: Her Majesty's Stationary Office; 1998.
19. Field A. *Discovering Statistics using SPSS*, 2nd edn. London: SAGE; 2005.
20. Farkas LG (editor). Examination. In: *Anthropometry of the Head and Face*. New York: Raven Press; 1994. pp. 3–56.
21. Tiddeman B, Duffy N, Rabey G. Construction and visualisation of three dimensional facial statistics. Computer Methods and Programmes. *Biostatistics* 2000;36: 9–20.
22. Bugaighis I. *3D facial morphometry in children with oral clefts*: Thesis, Newcastle upon Tyne: Newcastle University; 2009.
23. Hood CA. Three dimensional assessment of facial morphology in infants with cleft lip and palate. Thesis, University of Glascow. http://theses.gla.ac.uk/735/.
24. Shaw W et al. A six-centre international study of treatment outcome in patients with clefts of the lip and palate: part 5: general discussion and conclusions. *Cleft Palate Craniofac J* 1992;29:413–8.
25. Stauber I, Vairaktaris E, Holst A, Schuster M, Hirschfelder U, Neukam FW et al. Three dimensional analysis of facial symmetry in cleft lip and palate patients using optical surface data. *J Orofac Orthop* 2008;69: 268–82.
26. Duffy S, Noar J, Evans R, Sanders R. Three-dimensional Analysis of the child cleft face. *Cleft Palate Craniofac J* 2000;37:137–44.
27. Williams A, Shaw WC, Devlin HB. Provision of services for cleft lip and palate in England and Wales. *BMJ* 1994;309:1552.